Unwinding of the uniform lying helix structure in cholesteric liquid crystals next to a spatially uniform aligning surface

Patrick S. Salter,[1] Giovanni Carbone,[1] Sharon A. Jewell,[2] Steve J. Elston,[1] and Peter Raynes[1]
[1]*Department of Engineering Science, University of Oxford, Parks Road, Oxford OX1 3PJ, United Kingdom*
[2]*Electromagnetic Materials Group, School of Physics, University of Exeter, Stocker Road, Exeter EX4 4QL, United Kingdom*
(Received 3 August 2009; published 27 October 2009)

The symmetry of the cholesteric uniform lying helix (ULH) structure, where the helix axis is aligned in a single direction parallel to the device substrates, is not compatible with a uniform surface alignment and an unwinding of the helical structure is expected at the interface. Fluorescence confocal polarizing microscopy experiments are performed on the interface between a bulk ULH and a uniform aligning surface (for both planar and homeotropic alignments). The results are analyzed in the framework of a finite difference numerical simulation based on the Frank elastic distortion, to determine relevant director structures. An optical model is introduced to predict three-dimensional fluorescence profiles for the structures. Comparison of experimental and theoretical results shows that the equilibrium structure of the system involves a continuous unwinding of the helix close to the surface.

DOI: 10.1103/PhysRevE.80.041707 PACS number(s): 61.30.Eb, 61.30.Hn, 42.70.Df, 61.30.Dk

I. INTRODUCTION

The uniform lying helix (ULH) structure, where the helical axis of a chiral nematic is oriented in a single direction parallel to the confining substrates, is a development of the fingerprint texture, studied widely in long-pitch cholesterics [1]. The ULH structure has received recent attention in short pitch (sub ~500 nm) cholesterics for two distinct applications: to provide fast in-plane switching via the flexoelectro-optic effect for display technology [2–4] or alternatively as a medium supporting wavelength tunable photonic band edge lasing [5]. However, the ULH structure is neither stable nor easily aligned in standard device geometries, posing difficulties for any technological exploitation. Since the nematic director (the local average molecular orientation) continuously rotates along the helical axis, which is parallel to the confining walls, the ULH structure is not completely compatible with any uniform aligning surface. In the absence of external fields, the Grandjean structure, where the helix axis is orientated perpendicular to the substrates, is found to be the minimum energy configuration [6]. In the case of a chiral nematic with a positive dielectric anisotropy, the ULH texture can be formed by applying an electric field perpendicular to the device substrates. Even though this is a well known fact, the microscopic structure of the interface between a ULH texture and a uniform aligning layer is still not clear. If rigid boundary conditions are considered, two possible scenarios are predicted. The first one involves a half pitch periodic array of π disclination lines aligned perpendicular to the helical axis, facilitating the transition from the ULH to the substrate. The second scenario corresponds to a continuous unwinding of the cholesteric helix, such that the director field $\hat{\mathbf{n}}$ does not show any discontinuities. If p is the cholesteric pitch, the first scenario results in a $p/2$ periodic structure, but the second one has full pitch periodicity. This is due to the fact that continuous textures can only connect structures that are topologically equivalent. The spatially uniform director, which is present at the surface, has the same topology as a 2π, or full pitch, rotation of the director, while it has a distinct topology to a π, or half pitch, rotation.

A possible director field corresponding to the first scenario of a disclination mediated unwinding is shown in Fig. 1(a). Everywhere the twist distortion in the director field is in the same sense as the natural helicity of the medium. Figure 1(b) shows a possible director field for the continuous unwinding scenario. While this state avoids the large amount of

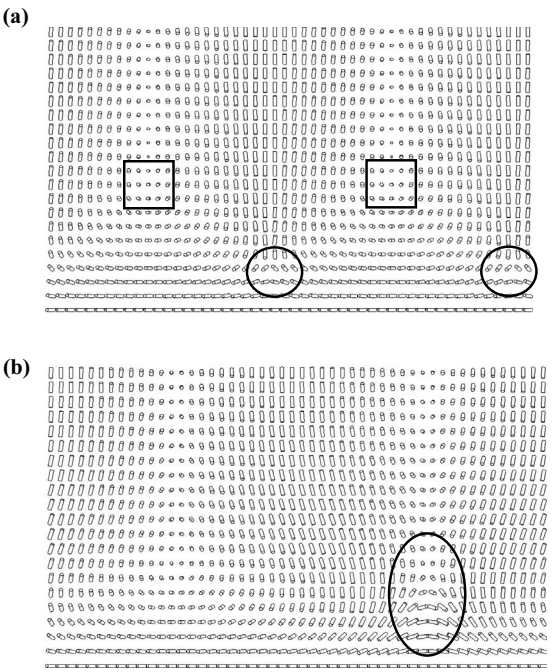

FIG. 1. Director plots for two possible transitions from a bulk ULH structure to a planar substrate. (a) The unwinding of the helix is facilitated by a $\tau^{-1/2}\lambda^{+1/2}$ disclination pair close to the substrate every half pitch [1]. The singular $\tau^{-1/2}$ disclinations are denoted by circles while the nonsingular $\lambda^{+1/2}$ disclinations are marked with squares. (b) An alternative situation is a smooth transition from the bulk helix to the planar substrate periodic over a full cholesteric pitch. This configuration avoids disclination formation but does require a region of twist in the opposite sense to the helix, which is ringed.

energy involved with the formation of the π disclination lines, it requires a region of twist in the opposite sense to that of the helix, invoking an associated high energy density. Therefore it is not obvious which mechanism will dominate, although this could be a key consideration when designing a device geometry with which to align and stabilize the ULH.

In this paper we address this question employing fluorescence confocal polarizing microscopy (FCPM) to image the interface between the bulk ULH and both planar and homeotropic aligning surfaces and analyzing the experimental data in the framework of a Frank elastic model. In Sec. II the FCPM is briefly introduced before reporting details on sample preparation and data acquisition in Sec. III. The acquired FCPM data are discussed in Sec. IV. The analysis of the data is reported in Sec. V, where the director field connecting a bulk ULH and a uniform aligning surface is predicted using a finite difference numerical simulation. An optical model is introduced, where a Jones routine [7] is employed to compensate for the effects of polarization rotation by the birefringent liquid crystal structure, allowing calculation of the fluorescence profiles for the simulated director configurations.

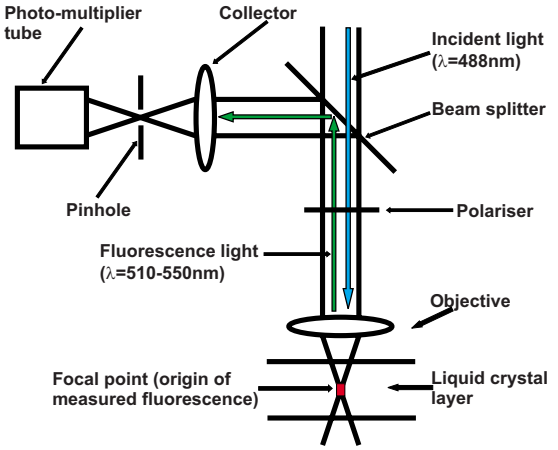

FIG. 2. (Color online) Schematic of the arrangement of optical components in a fluorescence confocal polarizing microscopy system. The polarizer ensures that only fluorescence light with the same polarization as the excitation beam passes through the setup to the photomultiplier tube, while the pinhole guarantees that the measured fluorescence originates only from the focal region of the excitation beam.

II. FLUORESCENCE CONFOCAL POLARIZING MICROSCOPY

A useful method for imaging a three dimensional director field is that of fluorescence confocal polarizing microscopy [8]. Cholesteric liquid crystals are an attractive option for study by FCPM thanks to the interesting three-dimensional director structures often observed. Previous studies on cholesterics have focused on defect structures in a Grandjean-Cano wedge device [9], surface and electric field frustrated fingers [10] and in-plane switching [11]. FCPM has additionally been employed in the investigation of Smectic A focal conic domains [8,12], drying droplets of DNA [13], nematic electrohydrodynamic convection [14] and liquid crystal colloid dispersions [15,16]. Here we exploit FCPM to reconstruct the director field at the interface between a bulk ULH structure and a spatially uniform surface, supplementing prior works on surface frustrated cholesteric stripes where the pitch p is of a similar magnitude to the device thickness d [17,18].

For the FCPM experiments, a low concentration of an anisotropic fluorescent dye is doped into the liquid crystal. The dye aligns with its long axis parallel to the liquid crystal director, although with potentially a different degree of order to that of the nematic host [19]. The sample is illuminated with a linearly polarized excitation beam of wavelength within the absorption band of the dye. If the transition dipole moment of the dye is parallel to its long molecular axis, absorption will be maximum when the excitation beam is polarized parallel to the director, and minimum when the polarization is perpendicular to the director. Given that the excitation lifetime of the dye is small [20], the subsequent fluorescence emission can also be assumed to be polarized parallel to the director. By analysis of the fluorescence emission with a polarizer parallel to that of the input beam, it is possible to infer the orientation of the director, the fluorescence intensity being proportional to $\cos^4\theta$, where θ is the angle between the director and the polarization of the incident light. By use of a confocal microscope, the pinhole in the optical set up (Fig. 2) ensures that only the emitted fluorescence from the volume of liquid crystal at the focus of the excitation beam reaches the detector. Thus information is gained on the director orientation within a volume of $\sim 1\ \mu m^3$ surrounding the focal spot, and by translation of the sample relative to the excitation beam it is possible to build up a three-dimensional image of the director configuration.

III. EXPERIMENT

The nematic liquid crystal used was MLC-15900–100, supplied by Merck, with dielectric anisotropy of $\Delta\epsilon=10.1$ and birefringence $\Delta n=0.091$. A small amount (0.01% w/w) of the anisotropic fluorescent dye *N*,*N*′8-Bis(2,5-di-*tert*-butylphenyl)-3,4,9,10-perylene dicarboximide (BTBP) from Sigma-Aldrich was added to the nematic for the FCPM measurements. Two different chiral mixtures were obtained by adding $\sim 1\%$ w/w and $\sim 0.5\%$ w/w of the chiral dopant CB15 to the nematic to create cholesterics of ~ 10 and $\sim 20\ \mu$m pitch, respectively. The relatively long chosen pitch lengths are required in order to resolve the interface structure of the ULH since the unwinding is expected to be realized over a distance smaller than the pitch. A lower limit for the unwinding depth δ is set by the dielectric coherence length $\xi_d=\sqrt{\frac{K}{\Delta\epsilon\epsilon_0}}\frac{1}{E}$ which provides a characteristic lengthscale for a distortion induced by an electric field E [21]. At the critical field for bulk dielectric unwinding of the helix $E_c=\frac{\pi^2}{p}\sqrt{\frac{K_2}{\Delta\epsilon\epsilon_0}}$, and $\xi_d=\sim\frac{p}{\pi^2}$. However, since the bulk and the surface have a different symmetry it is expected that δ might not be simply determined by ξ_d. An upper limit to δ is found from simulation of the director field

for the ULH next to uniform surface to be approximately equal to the cholesteric pitch [6], such that the depth of the unwinding region should be in the range $\xi_d < \delta \lesssim p$.

The experimental devices used comprised of two parallel glass plates separated by Mylar strips of thickness 70 μm and uniformly coated with the transparent conductor indium tin oxide. The ratio of device thickness d to chiral pitch p was chosen to correspond to that for devices containing short pitch materials intended for use in electro-optic applications. Therefore the confinement ratio $C=d/p$ is appreciably greater than unity, removing any potential of surface-induced frustration causing an unwinding of the helix [22]. To allow the use of a high numerical aperture oil-immersion objective the upper substrate was just 170 μm thick, while the lower substrate had a thickness of 1.1mm to add rigidity to the device. A polyimide (PI2555—Dupont) alignment layer was spin coated on to the lower substrate and rubbed to provide strong planar anchoring with a pretilt of $\sim 2°$. The interface between the ULH structure and the upper substrate was under investigation, and as such the upper substrate was spin-coated with either PI2555 and rubbed for planar alignment, or the surfactant N,N-dimethyl-n-octadecyl-3-aminopropyl-trimethoxysilyl chloride (DMOAP) for a homeotropic alignment.

The ULH structure was induced in the devices via two different procedures. In one approach the material was slowly cooled from the isotropic into the nematic phase with an oscillating (10 kHz) voltage applied, of magnitude just below the threshold for bulk dielectric unwinding of the helix. The orientation of the helix axis in the plane of the device is dictated by the alignment direction of the planar substrate, and the two were found to be nearly perpendicular. Alternatively the ULH was formed by applying an electric field to the Grandjean structure without any heating of the sample, creating a focal conic structure. Thereafter some flow was generated within the device by application of pressure to the top substrate in order to create a uniform in-plane alignment of the helix axis.

For investigation of the ULH surface interaction, the devices were mounted in an inverted confocal microscope system (Leica TCS SP5), operating in reflection mode, with the upper substrate (incident face) index matched to a 63× oil immersion lens (numerical aperture 1.4). An excitation wavelength of 488 nm was used and fluorescence light in the range 510–550 nm was collected. FCPM images were obtained from a 80×80 μm^2 region in the x-y plane in 0.2 μm steps through the cell, spanning a total distance of 80 μm in the z direction. Images were taken for the polarization of the excitation beam both parallel and perpendicular to the helix axis. For each set of data, image reconstruction software was used to compile the in-plane images and construct a cross section through the cell showing how the fluorescent intensity varies with depth.

IV. RESULTS

Figure 3 shows FCPM images of the interface between the ULH structure and a uniform planar substrate for the 20 μm pitch material. The ULH was formed by cooling from the isotropic to the nematic with an applied voltage of 10 V_{RMS} (corresponding to an electric field of ~ 0.14 V/μm). Image (a) corresponds to the polarization of the excitation beam perpendicular to the helix axis while in image (b) the polarization is parallel to it. Figure 3(a) clearly displays the ULH structure close to the substrate, alternate bands of high and low intensity indicating the fluorescent dye (and hence the director) is parallel and perpendicular to the substrate, respectively, in these regions. It can also be seen from Fig. 3 that the unwinding of the ULH next to the substrate appears to display a full pitch periodicity indicating that it involves a continuous distortion of the director. The fluorescence images in Fig. 3 also correspond well with those observed for cholesteric stripes parallel to the substrate alignment in surface frustrated thin planar devies [17,18]. In Fig. 3(a) the bright bands are not completely perpendicular to the substrate revealing that the helix axis is not indeed perfectly parallel to the substrates but slightly tilted. The intensity of the bright bands drops off sharply a distance of ~ 20 μm into the device, considerably less than the device thickness. This might suggest that the ULH structure is only existent adjacent to the substrate, and in the bulk the helix is unwound by the electric field and homeotoprically aligned. However the effect persisted across the entire voltage range, showing there to be little field dependence. Instead the observation is attributed to diffraction of the excitation beam by the periodic ULH structure, leading to significant aberration at the focus of the beam and a decrease in fluorescence intensity. Such an interpretation is further supported by experimental findings that the cut off depth in the device for ap-

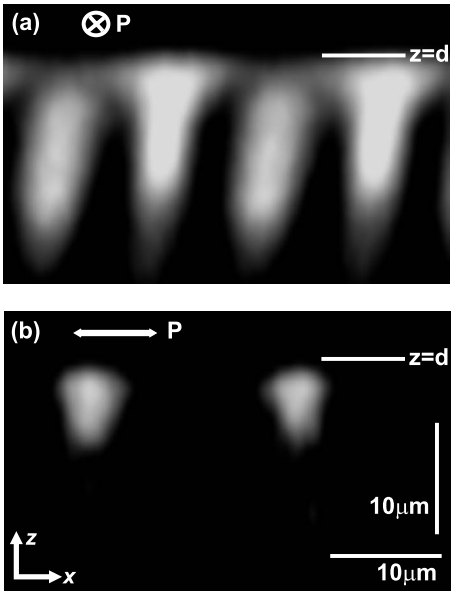

FIG. 3. FCPM images of the interface between a ULH bulk and a uniform planar substrate at $z=d$, with 10 V_{RMS} applied perpendicular to the surface and a chiral pitch of 20 μm. The ULH structure was formed by cooling from the isotropic to cholesteric phase with the field applied and the in-plane orientation of the helix is dictated by the surface alignment, for which the easy axis is in the y direction. The incident polarization of the laser is designated by **P** in each image, which is in (a) the y direction (perpendicular to the helix axis) and (b) the x direction (parallel to the helix).

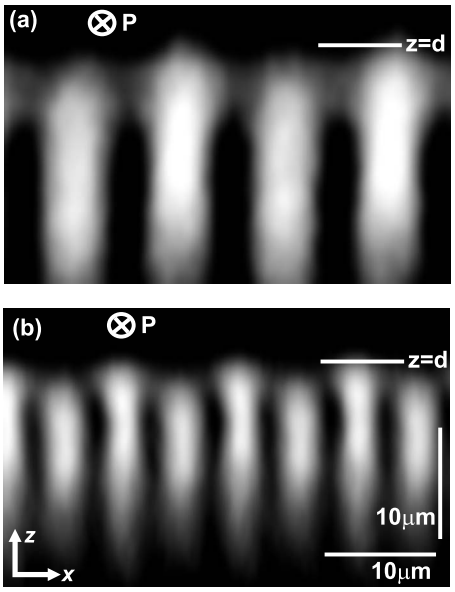

FIG. 4. FCPM images revealing the ULH structure near a uniform planar substrate at $z=d$, with the easy axis in the y direction. The polarization of the incident laser beam **P** is along the y direction (perpendicular to the helix axis) in each image. Image (a) shows the 20 μm pitch material in a ULH structure that was aligned by inducing flow within the device, with a voltage of 13.1 V_{RMS} applied perpendicular to the substrates. Image (b) shows the 10 μm pitch material in a ULH structure that was aligned by cooling from the isotropic with an applied voltage 20 V_{RMS}.

preciable fluorescence decreases with decreasing pitch length, the shorter period structure leading to an increase in diffractive aberration. When an objective lens with a lower numerical aperture was inserted, the cutoff depth was observed to increase, as might be expected since the decreased angular divergence in the beam will reduce the aberration.

The FCPM images in Figs. 4(a) and 4(b) also show the ULH structure aligned next to a planar substrate, with the polarization of the incident excitation beam perpendicular to the helix axis. Figure 4(a) features the same device considered in Fig. 3, although now the uniform orientation of the helix axis in the plane of the substrates was achieved by inducing flow within the device. In Fig. 4(b) the ULH was formed by cooling from the isotropic to the nematic, but with the shorter 10 μm pitch material. In both cases, an unwinding mechanism with full pitch periodicity is observed analogous to that discussed above in reference to Fig. 3. The images suggest that for both material pitches the unwinding of the ULH at the substrate is continuous in the director, independent of the procedure taken to form the ULH.

Figure 5 shows FCPM images representing the interaction of the ULH structure with a uniform homeotropic substrate for the 10 μm pitch material. The ULH was formed by application of 20 V_{RMS} between the substrates at room temperature, and flow was induced within the device to obtain a uniform in-plane orientation of the helix axis. It is again observed that the unwinding of the ULH next to the substrate displays a full pitch periodicity indicating that it involves a continuous distortion of the director.

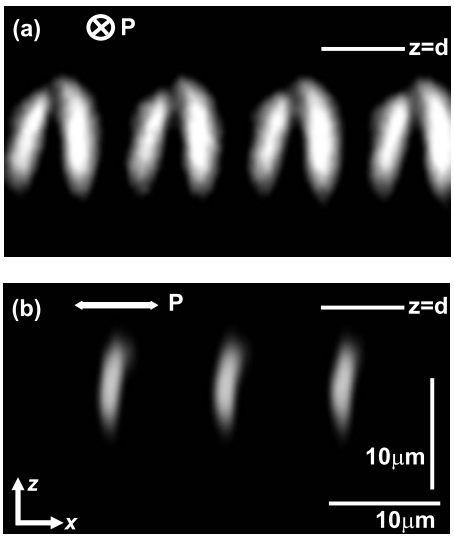

FIG. 5. FCPM images of the ULH structure near a uniform homeotropic substrate at $z=d$, when the incident polarization **P** of the laser is (a) perpendicular and (b) parallel to the helix axis. The material used had a pitch of $\sim$10 μm and there is 20 V_{RMS} applied between the substrates.

V. ANALYSIS

The recorded FCPM images of the ULH structure aligned next to a uniform surface all indicate a continuous distortion of the director in unwinding the helix, by virtue of the full pitch periodicity observed. However it is interesting to examine the interface in more detail and determine the relevant director field. This can be achieved by considering the bulk energy density for the system,

$$f(\hat{\mathbf{n}}) = \frac{1}{2}K_1[\nabla \cdot \hat{\mathbf{n}}]^2 + \frac{1}{2}K_2[\hat{\mathbf{n}} \cdot (\nabla \times \hat{\mathbf{n}}) + q]^2 + \frac{1}{2}K_3[\hat{\mathbf{n}} \times (\nabla \times \hat{\mathbf{n}})]^2 - \frac{1}{2}\epsilon_0 \Delta\epsilon(\hat{\mathbf{n}} \cdot \mathbf{E})^2, \quad (1)$$

where the first three terms describe the Frank elastic energy for splay, twist and bend director deformations, with respective elastic constants K_1, K_2, K_3 while $q=2\pi/p$ is the helical wave vector. The fourth term is related to the coupling of the dielectric polarization with the electric field E. The applied field in the experiment was oscillating at a frequency of 10 kHz, where dielectric interactions are expected to dominate over flexoelectric effects. Dielectric distortions in the director are identical for $\pm E$, whereas flexoelectric distortions are reversed for a change in field polarity. The response time for any flexoelectric reorientation is estimated to be considerably longer than the field period for this structure, and hence the flexoelectric coupling to the field is not included in the expression for the energy density.

We define a coordinate system where the z axis is perpendicular to the substrates, and the x axis parallel to the helix axis. A set of Euler-Lagrange equations is determined from the energy density [Eq. (1)] for three orthogonal components of the director n_x, n_y and n_z. These Euler-Lagrange equations are then solved on a regular grid using a simple relaxation

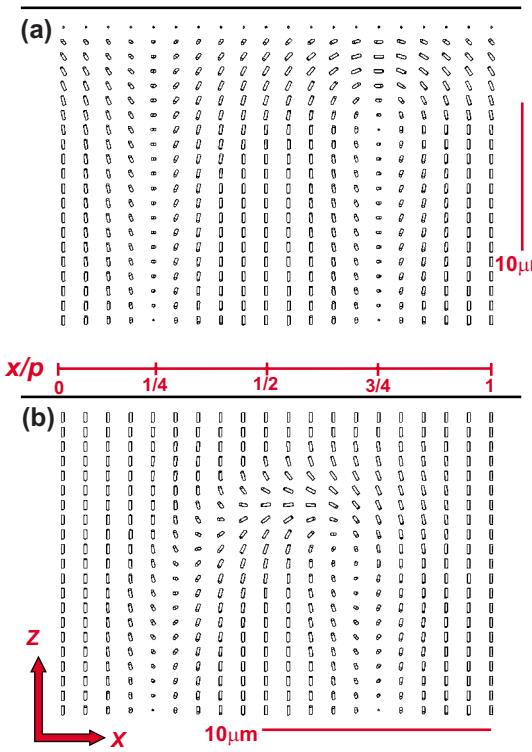

FIG. 6. (Color online) Calculated director structures for a continuous unwinding of the bulk ULH structure next to a substrate promoting uniform (a) planar and (b) homeotropic alignment. An electric field of 0.15 V/μm is applied perpendicular to the substrates. Lower electric fields result in an expansion of the unwinding region next to the substrate in the negative z direction. In (a) the helix axis is perpendicular to the substrate alignment direction, displaying a lesser degree of elastic distortion than the structure presented in Fig. 1(b).

method, minimizing the energy at each grid point and thus determining the director. Since the FCPM images strongly suggest a continuous distortion of the director, a finite difference approach with a Frank-Oseen director formulation of the free energy is applicable.

Cyclic boundary conditions are employed in the x direction and the width of the grid is equal to one natural pitch of the helix. The boundary condition at the top of the grid is for a substrate with uniform planar, or homeotropic, strong anchoring, while the bottom surface is initially set as the ULH structure and subsequently allowed to vary. Only the transition region where the ULH unwinds next to the substrate is investigated here, and the depth of the grid is equal to one full pitch of the helix. Simulations carried out for the full device thickness are found to give analogous results for the transition region, although computationally take considerably longer. A uniform electric field is applied perpendicular to the substrate, and as observed in experiment the structure relaxes to a Grandjean state when the field is omitted.

The calculated director structure for a material with 20 μm pitch and an applied electric field of 0.15 V/μm aligned adjacent to a uniform planar surface is shown in Fig. 6(a). The helix axis is perpendicular to the surface alignment direction, in contrast to the arrangement in Fig. 1(b), lowering the extent to which the structure has to twist in the opposite sense to the natural helicity of the medium. It should be noted however that the equilibrium angle between helix axis and substrate alignment is not always 90°, but depends on the applied electric field [23]. The depth of the unwinding region next to the substrate is increased for lower electric fields, potentially allowing a greater natural twist of the director perpendicular to the surface such that the bulk helix axis and the surface alignment direction are no longer perpendicular. Figure 6(b) shows the continuous unwinding of the ULH next to a uniform homeotropic substrate, also with a 20 μm pitch and an electric field of 0.15 V/μm. It is interesting to note the unwinding mechanism is very similar to that observed in the frustrated cholesteric fingers of type CF1 on a homeotropic alignment [10,24], and for cholesteric stripe patterns in surface frustrated thin samples [17,18].

One of the potential problems with FCPM is that the birefringence of the liquid crystal structure imaged may alter the input polarization of the excitation beam. Thus some care needs to be taken in the interpretation of the images, since a high fluorescence intensity does not necessarily correspond to regions where the director is parallel to the input polarization. The liquid crystal studied here has a relatively low birefringence of $\Delta n=0.091$, but reorientation of the input polarization should not be precluded, especially since the Mauguin parameter $\Delta np/2\lambda$ is of order unity, and hence a degree of polarization guiding is expected by any twisted structures [25]. Therefore when comparing the simulated director structures to the experimental images it would be useful to compensate for these effects. As such we include in our model a calculation of the polarization state of the excitation beam at each point in the structure in order to predict the fluorescence intensity.

Under the assumption that the excitation beam incident on the calculated director structures is a plane wave, a Jones matrix method is used to compute the change in polarization state $\mathbf{P}$ of the light as it propagates through the structure. The probability α of dye absorption is calculated at a point $\mathbf{r}$ in the structure by taking the square of the scalar product of the director and polarization state $\alpha=[\mathbf{P}(\mathbf{r})\cdot\hat{\mathbf{n}}(\mathbf{r})]^2$. Once excited, the probability $\beta(\theta)$ that a dye molecule emits the photon in a direction forming an angle θ with respect to the director orientation is proportional to $\sin^2\theta$ and the polarization of the photon is assumed to be in a plane containing the director. The emitted polarized light is propagated back to the analyzer, using the already mentioned Jones matrix method and only the component of the polarization parallel to the initial one is considered to contribute to the measured fluorescent intensity. Additionally a spatial average centered on $\mathbf{r}$ is applied when calculating the predicted fluorescence intensity taking into account the x and z dependence of the intensity of the excitation beam at the focus.

Figures 7 and 8 show predictions for the fluorescence intensity registered by FCPM next to planar and homeotropic aligning substrates, respectively. The images are obtained by carrying out the optics analysis described above on the director structures shown in Fig. 6. Good qualitative agreement with regard to the dimensions and positions of the fluorescence maxima is observed between the predicted images and the experimental measurements shown in Figs. 3 and 5, especially for the case of the ULH next to a surface inducing

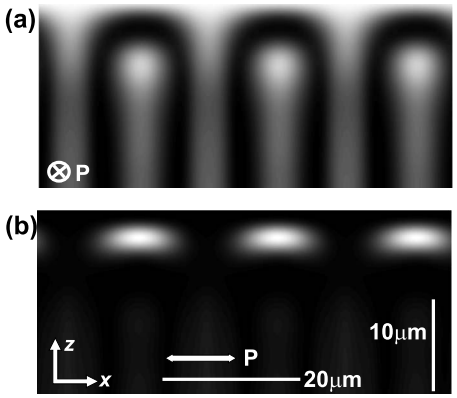

FIG. 7. Theoretical prediction of the FCPM images for the ULH unwinding continuously next to a substrate promoting uniform planar alignment with easy axis in the *y* direction. The images are calculated for the polarization state of the excitation beam **P** perpendicular (a) and parallel (b) to the helix axis.

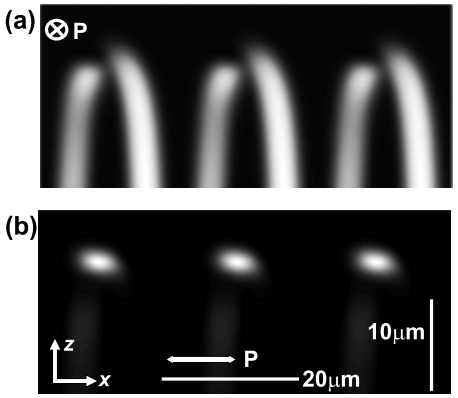

FIG. 8. Theoretical prediction of the FCPM images for the ULH unwinding continuously next to a substrate promoting uniform homeotropic alignment. The images are calculated for the polarization state of the excitation beam **P** perpendicular (a) and parallel (b) to the helix axis.

homeotropic alignment. A feature of particular importance in which there is good agreement in both sets of images is the director rotation perpendicular to the substrate with pitch periodicity. This is clearly visible in the recorded and predicted images [Figs. 3(b), 5(b), 7(b), and 8(b)] with the input polarization of the excitation beam parallel to the helix axis as a bright region near the surface once every pitch.

The optical model described provides only a first approximation for the effect of the birefringent liquid crystal layer on the incident polarization of the excitation beam. For high numerical aperture lenses, the incident light on the focal spot actually forms a cone of angle $\sim 67°$ (N.A.=1.4) and thus the assumption of an incident plane wave breaks down. In fact the path through the birefringent liquid crystal layer would need to be considered for rays from all these angles of incidence, additionally taking into account that the initial polarizations will not be collinear. The actual electric field corresponding to the excitation beam at the focal spot will be the integral of the electric field corresponding to all these individual rays. The calculation of this point-spread function becomes even more challenging due to the birefringent and inhomogeneous nature of the liquid crystal sample. In the future, work will be undertaken to further include these effects, although we note that the approximation made here still provides good qualitative agreement between the theoretical and experimental fluorescence profiles.

VI. CONCLUSION

We use fluorescence confocal polarizing microscopy to show that the interaction of the ULH structure with a surface promoting uniform alignment of the nematic director is facilitated by a continuous defect-free unwinding of the helix, in all cases for the long-pitch cholesteric system under observation. The presented optical model provides comparison between simulated director structures and experimental images, showing the two to be consistent. Some caution is required on extrapolating these results back to a situation involving the short pitch materials appropriate for electro-optic applications. While the device thickness, and minimum dielectric coherence length ξ_d prior to helix unwinding, are scaled in a manner analogous to the pitch, both the anchoring extrapolation length L and the nematic coherence length ξ_n remain constant [21]. The assumption of rigid anchoring is justified in our work since both the pitch p and the minimum dielectric coherence length ξ_d are a few orders of magnitude larger than the anchoring extrapolation length L, which for standard surface alignment materials is smaller than 100 nm. In the case of a chiral nematic with very short pitch and surface treated to produce weak alignment the situation can be different and director distortion at the surface can become important. The nematic coherence length gives the length scale of local order variation in the nematic phase and it is expected that a disclination mediated ULH surface interaction will become more applicable as the magnitude of ξ_d approaches that of ξ_n. Such an effect is impossible to probe by the method of FCPM since the long-pitch materials are required in order to resolve the surface unwinding of the helix. Recent observations by polarizing optical microscopy suggest that both unwinding mechanisms are realized in short pitch materials, dependent on the electric field applied during formation of the ULH [26]. In such circumstances the director distortion at the surface for the continuous unwinding transition will still be of the form presented in Fig. 6. In conclusion, we believe that providing greater insight into the basic alignment characteristics of the helix next to a surface will aid the design of device geometries that might optimize the stability and electro-optic applicability of the interesting ULH structure.

ACKNOWLEDGMENTS

The authors would like to thank the Engineering and Physical Sciences Research Council (U.K.) and Merck for financial support.

[1] P. Cladis and M. Kleman, Mol. Cryst. Liq. Cryst. **16**, 1 (1972).
[2] P. Rudquist, M. Buivydas, L. Komitov, and S. T. Lagerwall, J. Appl. Phys. **76**, 7778 (1994).
[3] B. J. Broughton, M. J. Clarke, S. M. Morris, A. E. Blatch, and H. J. Coles, J. Appl. Phys. **99**, 023511 (2006).
[4] G. Carbone, P. Salter, S. J. Elston, P. Raynes, L. D. Sio, S. Ferjani, G. Strangi, C. Umeton, and R. Bartolino, Appl. Phys. Lett. **95**, 011102 (2009).
[5] G. Strangi, V. Barna, R. Caputo, A. de Luca, C. Versace, N. Scaramuzza, C. Umeton, R. Bartolino, and G. N. Price, Phys. Rev. Lett. **94**, 063903 (2005).
[6] P. S. Salter, S. J. Elston, and E. P. Raynes (unpublished).
[7] R. C. Jones, J. Opt. Soc. Am. **31**, 488 (1941).
[8] I. I. Smalyukh, S. V. Shiyanovskii, and O. D. Lavrentovich, Chem. Phys. Lett. **336**, 88 (2001).
[9] I. I. Smalyukh and O. D. Lavrentovich, Phys. Rev. E **66**, 051703 (2002).
[10] I. I. Smalyukh, B. I. Senyuk, P. Palffy-Muhoray, O. D. Lavrentovich, H. Huang, E. C. Gartland, V. H. Bodnar, T. Kosa, and B. Taheri, Phys. Rev. E **72**, 061707 (2005).
[11] S. A. Jewell and J. R. Sambles, Phys. Rev. E **78**, 012701 (2008).
[12] J. P. Bramble, S. D. Evans, J. R. Henderson, T. J. Atherton, and N. J. Smith, Liq. Cryst. **34**, 1137 (2007).
[13] I. I. Smalyukh, O. V. Zribi, J. C. Butler, O. D. Lavrentovich, and G. C. L. Wong, Phys. Rev. Lett. **96**, 177801 (2006).
[14] N. Gheorghiu, I. I. Smalyukh, O. D. Lavrentovich, and J. T. Gleeson, Phys. Rev. E **74**, 041702 (2006).
[15] O. P. Pishnyak, S. Tang, J. R. Kelly, S. V. Shiyanovskii, and O. D. Lavrentovich, Phys. Rev. Lett. **99**, 127802 (2007).
[16] A. Jakli, B. Senyuk, G. Liao, and O. D. Lavrentovich, Soft Matter **4**, 2471 (2008).
[17] I. I. Smalyukh, Mol. Cryst. Liq. Cryst. **477**, 23 (2007).
[18] S. V. Shiyanovskii, I. I. Smalyukh, and O. D. Lavrentovich, *Defects in Liquid Crystals: Computer Simulations, Theory and Experiment*, edited by O. D. Lavrentovich, P. Pasini, C. Zannoni, and S. Zumer (Kluwer Academic Publishers, Dordrecht, 2001).
[19] J. Constant, E. P. Raynes, I. A. Shanks, D. Coates, G. W. Gray, and D. G. McDonnell, J. Phys. D: Appl. Phys. **11**, 479 (1978).
[20] W. E. Ford and P. V. Kamat, J. Phys. Chem. **91**, 6373 (1987).
[21] P. G. de Gennes and J. Prost, *The Physics of Liquid Crystals* (Oxford University Press, New York, 1993).
[22] P. Oswald, J. Baudry, and S. Pirkl, Phys. Rep. **337**, 67 (2000).
[23] S. D. Lee and J. S. Patel, Phys. Rev. A **42**, 997 (1990).
[24] J. Baudry, S. Pirkl, and P. Oswald, Phys. Rev. E **57**, 3038 (1998).
[25] C. H. Gooch and H. A. Tarry, J. Phys. D **8**, 1575 (1975).
[26] P. S. Salter, S. J. Elston, E. P. Raynes, and L. A. Parry-Jones, Jpn. J. Appl. Phys. **48**, 101302 (2009).